

Ion-Selective Uptake

International Edition: DOI: 10.1002/anie.201511633
German Edition: DOI: 10.1002/ange.201511633

Reduction-Induced Highly Selective Uptake of Cesium Ions by an Ionic Crystal Based on Silicododecamolybdate

Saori Seino, Ryosuke Kawahara, Yoshiyuki Ogasawara, Noritaka Mizuno, and Sayaka Uchida*

Abstract: Cation adsorption and exchange has been an important topic in both basic and applied chemistry relevant to materials synthesis and chemical conversion, as well as purification and separation. Selective Cs^+ uptake from aqueous solutions is especially important because Cs^+ is expensive and is contained in radioactive wastes. However, the reported adsorbents incorporate Rb^+ as well as Cs^+ , and an adsorbent with high selectivity toward Cs^+ has not yet been reported. Highly selective uptake of Cs^+ by an ionic crystal $(\text{etpyH})_2[\text{Cr}_3\text{O}(\text{OOCH})_6(\text{etpy})_3]_2[\alpha\text{-SiMo}_{12}\text{O}_{40}]\cdot 3\text{H}_2\text{O}$ (etpy = 4-ethylpyridine) is described. The compound incorporated up to $3.8\text{ mol}(\text{Cs}^+)\text{mol}(\text{s})^{-1}$ (where s = solid) by cation-exchange with etpyH^+ and reduction of silicododecamolybdate with ascorbic acid. The amount of Cs^+ uptake was comparable to that of Prussian blue, which is widely recognized as a good Cs^+ adsorbent. Moreover, other alkali-metal and alkaline-earth-metal cations were almost completely excluded ($< 0.2\text{ mol}(\text{s})^{-1}$).

Selective adsorption and ion-exchange of alkali-metal cations from aqueous solutions has been an important topic in both basic and applied chemistry relevant to material synthesis and chemical conversion, as well as purification and separation.^[1] A classic example is the gas adsorption properties of microporous Linde Type A (LTA-type) zeolites, which can be modified by the types of counter-cations used because electrostatic host–guest interactions as well as average pore sizes are altered on cation adsorption.^[2] These zeolites are also used as alkali-metal cation exchangers,^[3] showing selectivity for Na^+ and K^+ (but less so for Cs^+), which is in line with the ionic radius of alkali-metal cations^[4] (Na^+ 1.02 \AA $<$ K^+ 1.38 \AA $<$ Rb^+ 1.52 \AA $<$ Cs^+ 1.67 \AA). On the other hand, acidic zeolites show the reverse selectivity (Na^+ , K^+ $<$ Cs^+),^[5] which is in line with the hydration radius^[6] (Na^+ 3.58 \AA $>$ K^+ 3.31 \AA \approx Rb^+ 3.29 \AA \approx Cs^+ 3.29 \AA) and Gibbs energy of dehydration^[7] (Na^+ 424 kJ mol^{-1} $>$ K^+ 352 kJ mol^{-1} $>$ Rb^+

329 kJ mol^{-1} $>$ Cs^+ 306 kJ mol^{-1}) of alkali-metal cations. A possible explanation for the observed reverse selectivity follows: a strong electrostatic field is generated by acidic protons and/or the conjugate base (typically O^{2-}), which facilitates adsorption of water.^[8] Therefore, alkali-metal cations in acidic zeolites are normally hydrated so that a cation with a low degree of hydration can diffuse more easily. However, sizes and physical properties of Rb^+ and Cs^+ are so similar that discrimination of Cs^+ from Rb^+ is a very challenging task.

Selective Cs^+ uptake from aqueous solutions is especially important because Cs^+ is expensive and is contained in radioactive wastes.^[9] Besides zeolites, Prussian blues^[10] and layered compounds^[11] have been researched and applied as Cs^+ adsorbents. Prussian blue, which is a classical coordination polymer with general formula $[\text{Fe}^{\text{III}}_4[\text{Fe}^{\text{II}}(\text{CN})_6]_3]$, captures Cs^+ with high selectivity compared to Na^+ and K^+ because of physical adsorption with an anion or chemical adsorption by lattice defect.^[10b] Among layered compounds, $\text{K}_{2x}\text{Mn}_x\text{Sn}_{3-x}\text{S}_6$ shows high Cs^+ uptake over a wide pH range because of soft Lewis acid–base interactions ($\text{Cs}^+\cdots\text{S}^{2-}$).^[11b] However, these materials adsorb Rb^+ as well as Cs^+ , and an adsorbent with high selectivity toward Cs^+ has not yet been reported.

Polyoxometalates (POMs) are nano-sized anionic metal–oxygen clusters of early transition metals and have stimulated research in broad fields of sciences.^[12] In particular, redox-active Keggin-type polyoxomolybdates $[\alpha\text{-XMo}_{12}\text{O}_{40}]^{n-}$ (X = P, Si) have been applied as oxidation catalysts and molecular cluster batteries.^[13,14] Recently, we reported a redox-active ionic crystal composed of $[\alpha\text{-PMo}_{12}\text{O}_{40}]^{3-}$ and a macrocation $[\text{Cr}_3\text{O}(\text{OOCH})_6(\text{mepy})_3]^+$ (mepy = 4-methylpyridine).^[15] The compound possessed one-dimensional open channels, which showed cooperative migration of electrons with alkali-metal cations. However, cation uptake by this compound was non-selective, and $2.0\text{ mol}(\text{K}^+/\text{Rb}^+/\text{Cs}^+)\text{mol}(\text{s})^{-1}$ (s = solid) was captured.

Herein, synthesis of an ionic crystal $(\text{etpyH})_2[\text{Cr}_3\text{O}(\text{OOCH})_6(\text{etpy})_3]_2[\alpha\text{-SiMo}_{12}\text{O}_{40}]\cdot 3\text{H}_2\text{O}$ (**I-as**; etpy = 4-ethylpyridine, etpyH^+ = 4-ethylpyridinium ion) with closed pores is described.^[16] Compound **I-as** incorporated up to $3.8\text{ mol}(\text{Cs}^+)\text{mol}(\text{s})^{-1}$ by cation-exchange with etpyH^+ and reduction of silicododecamolybdate $[\alpha\text{-SiMo(VI)}_{12}\text{O}_{40}]^{4-}$ into $[\alpha\text{-SiMo(V)}_n\text{Mo(VI)}_{12-n}\text{O}_{40}]^{(4+n)-}$ with ascorbic acid. Other alkali-metal (Na^+ , K^+ , and Rb^+) and alkaline-earth-metal (Mg^{2+} , Ca^{2+} , Sr^{2+} , and Ba^{2+}) cations were almost completely excluded ($< 0.2\text{ mol}(\text{s})^{-1}$).

Yellow–brown crystals of **I-as** were obtained at the interface of a 1,2-dichloroethane solution with $[\text{Cr}_3\text{O}(\text{OOCH})_6(\text{etpy})_3]^+$ and a methanol solution containing

[*] S. Seino, R. Kawahara, Dr. S. Uchida
Department of Basic Science, School of Arts and Sciences,
The University of Tokyo
3-8-1 Komaba, Meguro-ku, Tokyo 153-8902 (Japan)
E-mail: csayaka@mail.ecc.u-tokyo.ac.jp

Dr. S. Uchida
JST-PRESTO
4-1-8 Honcho, Kawaguchi, Saitama 332-0012 (Japan)

Dr. Y. Ogasawara, Prof. N. Mizuno
Department of Applied Chemistry, School of Engineering,
The University of Tokyo
7-3-1 Hongo, Bunkyo-ku, Tokyo 113-8656 (Japan)

Supporting information for this article can be found under <http://dx.doi.org/10.1002/anie.201511633>.

$[\alpha\text{-SiMo}_{12}\text{O}_{40}]^{4-}$. IR spectra of **I-as** confirmed that the molecular structures of POM and macrocation were maintained (Supporting Information, Figure S2). Single-crystal X-ray diffraction (XRD) analysis of **I-as** showed that one POM and two macrocations were arranged alternately along the *a*-axis (Figure 1 a), while two etpyH^+ ions counterbalance

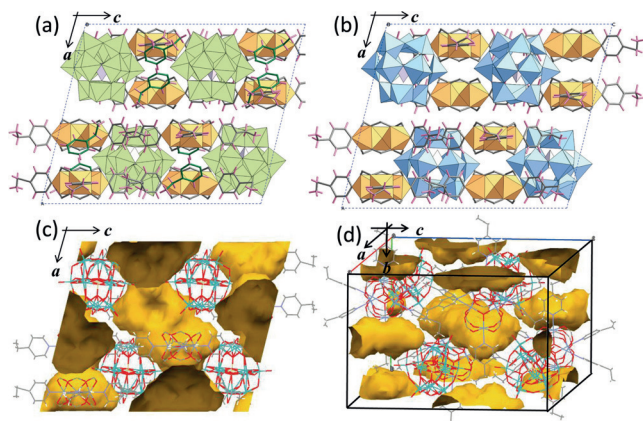


Figure 1. a) Crystal structure of **I-as**. b) A model structure of **I-red** constructed by removing one of the three etpy ligands in the macrocation and the etpyH^+ ion from (a). c) and d) Void analysis of **I-red** with a probe radius of 1.2 Å viewed from different directions. Green and blue polyhedra show the $[\text{MoO}_6]$ units of fully oxidized and reduced POM, respectively. Orange and purple polyhedra show the $[\text{CrO}_5\text{N}]$ units of macrocation and $[\text{SiO}_4]$ units of POM, respectively. Aromatic rings of etpy ligands of the macrocation and etpyH^+ are drawn in gray and green, respectively. In (c) and (d), void spaces are shown in brown. Each void has a size of about 6.5 by 12.5 Å.

the anion charge. The etpyH^+ ions were located in the vicinity of POMs with $\text{N(H)}\text{--O}$ distances of 2.668 and 2.726 Å. Void analysis (probe radius 1.2 Å) showed that the crystal structure of **I-as** is basically non-porous (void volume is 1.9% of the unit cell). Thermogravimetry showed that **I-as** contained 3 $\text{mol(H}_2\text{O)}\text{mol(I-as)}^{-1}$ (Supporting Information; Figure S3). The results of elemental analysis of **I-as** using inductively coupled plasma (ICP), atomic absorption spectrometry (AAS), and combustion techniques, are shown in Table 1.

The etpyH^+ ion contained inside **I-as** could be exchanged with Cs^+ by treatment with an aqueous solution of CsCl at 343 K.^[17–19] Elemental analysis showed that etpyH^+ was completely exchanged with Cs^+ and that etpy of the macrocation was partially exchanged with H_2O (Table 1).^[20] The Cs^+ -exchanged compound is denoted **I-IE** hereafter (IE = ion-exchange). Ion-exchange with other alkali-metal and alkaline-earth-metal cations hardly proceeded under the same conditions ($< 0.15 \text{ mol mol(s)}^{-1}$; Supporting Information, Table S1).

To increase the amount of Cs^+ uptake, reduction-induced ion-exchange was carried out. By this method, ascorbic acid was added as a reducing reagent to an aqueous solution of CsCl and **I-as** at 343 K.^[21] The yellowish-brown crystals of **I-as** became blue, suggesting reduction of the POM. The degree of reduction will be discussed later. The reduction-induced ion-exchange compound is denoted **I-red** hereafter (red = reduction).^[19] Elemental analysis showed that

Table 1: Elemental analysis (calcd %).^[a]

	C	H	N	Cr	Cs	Mo	Si
$(\text{etpyH})_2[\text{Cr}_3\text{O}(\text{OOCH})_6(\text{etpy})_3]_2[\alpha\text{-SiMo}_{12}\text{O}_{40}] \cdot 3 \text{H}_2\text{O}$							
I-as	22.03 (22.48)	2.49 (2.55)	2.88 (3.08)	8.50 (8.59)	0.00 (0.00)	31.76 (31.70)	0.77 (0.77)
$\text{Cs}_2[\text{Cr}_3\text{O}(\text{OOCH})_6(\text{etpy})_{2.5}(\text{H}_2\text{O})_{0.5}]_2[\alpha\text{-SiMo}_{12}\text{O}_{40}] \cdot 7 \text{H}_2\text{O}$							
I-IE	14.46 (15.39)	2.16 (2.06)	1.98 (1.91)	8.23 (8.51)	8.03 (7.25)	32.27 (31.40)	0.71 (0.77)
$\text{Cs}_{3.8}\text{H}_{3.0}[\text{Cr}_3\text{O}(\text{OOCH})_6(\text{etpy})_2(\text{H}_2\text{O})_2]_2[\alpha\text{-SiMo}_{12}\text{O}_{40}] \cdot 5 \text{H}_2\text{O}$							
I-red	12.45 (12.76)	1.45 (1.74)	1.56 (1.49)	7.93 (8.28)	13.23 (13.41)	30.69 (30.57)	0.82 (0.77)
$\text{Cs}_{3.8}\text{H}_{0.2}[\text{Cr}_3\text{O}(\text{OOCH})_6(\text{etpy})_2(\text{H}_2\text{O})_2]_2[\alpha\text{-SiMo}_{12}\text{O}_{40}] \cdot 5 \text{H}_2\text{O}$							
I-ox	12.34 (12.77)	1.51 (1.66)	1.47 (1.49)	8.85 (8.29)	13.41 (13.42)	30.71 (30.60)	0.74 (0.75)

[a] Carbon, hydrogen, and nitrogen were analyzed by combustion analysis; cesium was analyzed by AAS; chromium, molybdenum, and silicon were analyzed by ICP.

3.8 $\text{mol(Cs}^+)\text{mol(I-red)}^{-1}$ was incorporated by ion-exchange and reduction, and that etpy of the macrocation was partially exchanged with H_2O (Table 1).^[20] The amount of Cs^+ uptake per gram of adsorbent (134 mg g^{-1}) was comparable to that of Prussian blue^[10b] (133 mg g^{-1}), which is widely recognized as a good Cs^+ adsorbent. Redox-induced ion-exchange with other alkali-metal and alkaline-earth-metal cations hardly proceeded under the same conditions ($< 0.2 \text{ mol mol(s)}^{-1}$).

Equilibrium amounts of Cs^+ uptake as a function of initial Cs^+ concentration of the aqueous solution are shown in Figure 2a (reduction-induced ion-exchange method). The amounts of Cs^+ uptake increased with Cs^+ concentration, and saturation was reached at 151 mmol L^{-1} . Figure 2b shows the time course of Cs^+ uptake (200 mmol L^{-1}). The experimental data was reproduced well by Fick's diffusion equation in the radial direction^[22] with an average particle size of 10 μm (SEM images; Supporting Information, Figure S4) and a diffusion coefficient of $8.2 \times 10^{-12} \text{ cm}^2 \text{ s}^{-1}$, suggesting that Cs^+ is uniformly distributed in the particles.

Oxidation of **I-red** was carried out with aqueous chlorine solution as an oxidizing reagent.^[23] Blue crystals of **I-red** gained a yellow hue, suggesting partial oxidation of the POM. The oxidized compound is denoted **I-ox** hereafter (ox = oxidation). Elemental analysis showed that **I-ox** also contained 3.8 $\text{mol(Cs}^+)\text{mol(s)}^{-1}$ and that Cs^+ is not released into the

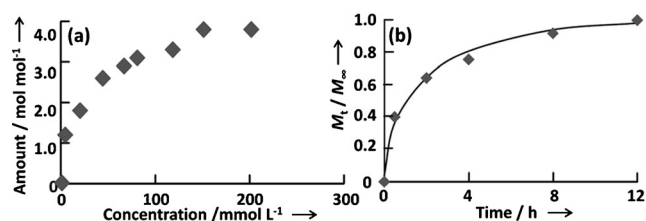


Figure 2. a) Equilibrium amounts of Cs^+ uptake versus initial Cs^+ concentration of the aqueous solution. b) Time-course of Cs^+ uptake ($\text{Cs}^+ = 200 \text{ mmol L}^{-1}$). The solid line shows the calculation according to Fick's law of diffusion.

solution by oxidation (Table 1). Therefore, **I-as** is potentially suitable for capturing radioactive Cs^+ in seawater that contains large amounts of alkali-metal and alkaline-earth-metal cations. Competitive uptake of Cs^+ from binary mixtures ($A^+/\text{Cs}^+ = 1$, where $A = \text{Na}, \text{K}$, and Rb ; $B^{2+}/\text{Cs}^+ = 0.5$, where $B = \text{Mg}, \text{Ca}, \text{Sr}$, and Ba ; $C^+/\text{Cs}^+ = 10$, where $C = \text{Na}$ and Rb) showed $>94\%$ selectivity for Cs^+ (see Supporting Information for results with low Cs^+ concentration). Notably, Cs^+ uptake only increased slightly to $4.1 \text{ mol}(\text{Cs}^+) \text{ mol}(\text{s})^{-1}$ by a redox-induced ion-exchange treatment of **I-ox**, suggesting that the saturation amount is about $4 \text{ mol}(\text{Cs}^+) \text{ mol}(\text{s})^{-1}$.

Powder XRD patterns of **I-as**, **I-IE**, **I-red**, and **I-ox** were essentially the same, showing that the arrangement of anions and cations in **I-as** is maintained during the redox process (Figure 3). According to this result, a model structure of **I-red**

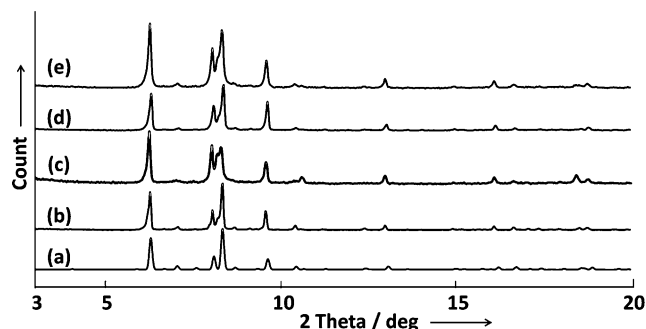


Figure 3. Powder XRD patterns of a) **I-as** (calculated), b) **I-as**, c) **I-IE**, d) **I-red**, and e) **I-ox**.

was constructed by removing one of the three etpy ligands in the macrocation^[20] and etpyH^+ from the crystal structure of **I-as** (Figure 1b). Void analysis (probe radius 1.2 \AA) of the model structure of **I-red** was carried out, and the results are shown in Figures 1c (*ac*-plane) and 1d (a view allowing observation of closed pores). The compound possessed closed pores with a size of approximately 6.5 by 12.5 \AA , and the void volume was 13.7% (1467 \AA^3) of the unit cell.

The degrees of reduction of POM in **I-red** and **I-ox** were investigated. A UV/Vis spectrum of **I-red** showed a broad band around 14000 cm^{-1} resulting from the inter-valence charge-transfer (IVCT) between Mo^V and Mo^{VI} ,^[24] which was not observed in **I-as** (Supporting Information, Figure S5). Wide-scan X-ray photoelectron spectroscopy (XPS) of **I-as**, **I-red**, and **I-ox** confirmed the absence of Cs^+ in **I-as**, and the existence of Cs^+ in **I-red** and **I-ox** (Supporting Information, Figure S6). Figure 4a shows the narrow-scan XPS spectrum of **I-red** in the Mo 3d region ($3d_{5/2}$ and $3d_{3/2}$) together with the result of peak deconvolution, which was carried out according to the method in Ref. [25]. The reduced Mo^V fraction in **I-red** was 40% , suggesting a 4.8 electron reduction of the POM.^[26] Therefore, **I-red** can be formulated as $\text{Cs}_{3.8}\text{H}_{3.0}[\text{Cr}_3\text{O}(\text{OOCH})_6(\text{etpy})_2(\text{H}_2\text{O})]_2[\alpha\text{-SiMo(V)}_{4.8}\text{Mo(VI)}_{7.2}\text{O}_{40}]\cdot 5\text{H}_2\text{O}$, and three protons were added to compensate for the anion charge (Table 1).^[27] The XPS spectrum of **I-ox** showed that the reduced Mo^V fraction was 17% (Supporting Information, Figure S8). Considering that Cs^+ is not released by oxidation, **I-ox** can be formulated as $\text{Cs}_{3.8}\text{H}_{0.2}[\text{Cr}_3\text{O}(\text{OOCH})_6(\text{etpy})_2\cdot$

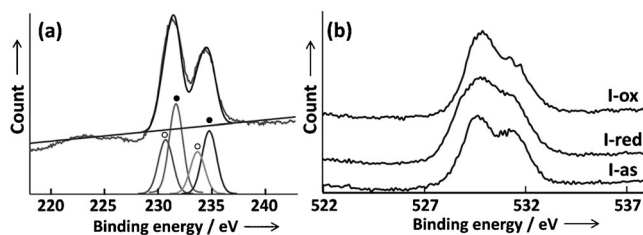


Figure 4. a) XPS spectrum of **I-red** in the Mo 3d region (upper). Peaks at the lower and higher energies correspond to $\text{Mo } 3d_{5/2}$ and $3d_{3/2}$ components, respectively. Deconvolution results are shown below the spectrum. Within each peak, lines at the lower (○) and higher (●) energies indicate Mo^V and Mo^{VI} species, respectively. b) XPS spectra of **I-as**, **I-red**, and **I-ox** in the O 1s region.

$(\text{H}_2\text{O})]_2[\alpha\text{-SiMo(V)}_{2.0}\text{Mo(VI)}_{10.0}\text{O}_{40}]\cdot 5\text{H}_2\text{O}$. These results show that protons, rather than Cs^+ , are released into the solution by the oxidation treatment. Figure 4b shows the narrow-scan XPS spectra of **I-as**, **I-red**, and **I-ox** in the O 1s region. Peaks around 531 eV and 530 eV are assigned to the formic oxygen of the macrocation and oxygen of POM, respectively.^[28] The low-energy peak is broadened by reduction, which can be explained by the localization of electrons on the Mo-O-Mo oxygen atom during IVCT.^[29]

The bar graph in Figure 5a summarizes the amounts of Cs^+ uptake in **I-IE** ($2.0 \text{ mol}(\text{Cs}^+) \text{ mol}(\text{I-IE})^{-1}$), **I-red** ($3.8 \text{ mol}(\text{Cs}^+) \text{ mol}(\text{I-red})^{-1}$), and **I-ox** ($3.8 \text{ mol}(\text{Cs}^+) \text{ mol}(\text{I-ox})^{-1}$) together with their photographic images.^[30] The bar graph in Figure 5b summarizes the amounts of various cations incorporated into **I-as** by the reduction-induced ion-exchange method ($<0.2 \text{ mol} \text{ mol}(\text{s})^{-1}$ for ions other than Cs^+). These results show that both high capacity and selectivity toward Cs^+ is attained.

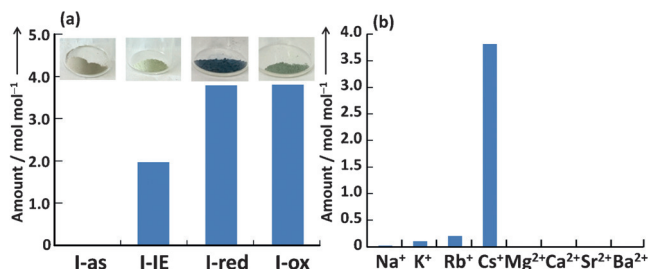


Figure 5. a) Amounts of Cs^+ uptake in **I-IE**, **I-red**, and **I-ox**, and their photographic images (including **I-as**). b) Amounts of various cations incorporated into **I-as** by the reduction-induced ion-exchange method.

As stated above, hydration radii and Gibbs energy of dehydration of alkali-metal cations decreases in the order $\text{Na}^+ > \text{K}^+ > \text{Rb}^+ > \text{Cs}^+$.^[6,7] Therefore, it is more facile to remove the water of hydration from Cs^+ , thereby allowing the ion to more easily enter and diffuse through the crystal lattice. The coulomb interaction between Cs^+ and POM oxygen atoms in **I-red** was estimated to be -310 kJ mol^{-1} with an average Mulliken charge of $-0.7e$ ^[31] in aqueous media, and a combined Cs^+ and O^{2-} ionic radius^[4] of 3.1 \AA , which may be large enough to compensate for the dehydration energy of Cs^+ (306 kJ mol^{-1}).^[7] The diffusion coefficient (Figure 2b)

was much smaller than those of conventional Cs^+ adsorbents, such as bentonite clay ($10^{-9} \text{ cm}^2 \text{ s}^{-1}$),^[11a] probably because the pores are closed. Notably, an ionic crystal composed of $[\text{Cr}_3\text{O}(\text{OOCH})_6(\text{mepy})_3]^+$ instead of $[\text{Cr}_3\text{O}(\text{OOCH})_6(\text{etpy})_3]^+$ possessed one-dimensional open channels,^[16] and this compound could incorporate Na^+ ($2.5 \text{ mol}(\text{Na}^+) \text{ mol}(\text{s})^{-1}$) as well as Cs^+ ($3.5 \text{ mol}(\text{Cs}^+) \text{ mol}(\text{s})^{-1}$) by the reduction-induced ion-exchange method. Based on these results and considerations, high selectivity towards Cs^+ is a result of the existence of closed pores rather than open channels. Additionally, flexibility of the crystal lattice caused by isotropic and long-range Coulomb interactions among the constituent ions,^[32] may have contributed to diffusion of Cs^+ between the closed pores.

Finally, instead of using reducing reagents, reduction-induced ion-exchange was carried out under UV/Vis irradiation ($\lambda > 250 \text{ nm}$) with methanol as a solvent and a sacrificing reagent (Supporting Information, Figure S9). The reaction proceeded smoothly, and preliminary results showed a more than 50% increase in Cs^+ uptake, which probably results from suppressed H^+ uptake. Further studies on the photochemical method will be reported in due course.

Experimental Section

Synthesis of **I-as**: $[\text{Cr}_3\text{O}(\text{OOCH})_6(\text{etpy})_3](\text{ClO}_4) \cdot n\text{H}_2\text{O}$ ^[33] (0.7 g, 0.5 mmol) was dissolved in 1,2-dichloroethane (100 mL), and the solution filtered to remove impurities (solution A). $\text{H}_4[\alpha\text{-SiMo}_{12}\text{O}_{40}] \cdot n\text{H}_2\text{O}$ ^[34,35] (0.8 g, 0.25 mmol) was dissolved in methanol (20 mL), and the solution filtered to remove impurities (solution B). Solution B was layered on top of solution A, and yellowish-brown crystals of **I-as** were formed at the interface within a few days (yield 40%). Synthesis of $\text{K}_2[\text{Cr}_3\text{O}(\text{OOCH})_6(\text{mepy})_3]_2[\alpha\text{-SiMo}_{12}\text{O}_{40}] \cdot n\text{H}_2\text{O}$ (Supporting Information, Figure S1) was carried out by the same method as **I-as** except for the addition of CH_3COOK into solution B. Otherwise no crystals were obtained.

Single-crystal X-ray structure analyses: X-ray diffraction data of **I-as** were collected at 93 K with a CCD 2D detector using a Rigaku Mercury diffractometer with graphite-monochromated MoK_α radiation ($\lambda = 0.71069 \text{ \AA}$). The structures were solved by direct methods (SHELX97), expanded by Fourier techniques, and refined by full-matrix least-squares against F^2 with the SHELXL package. Chromium, oxygen, and nitrogen atoms of the macrocation were refined anisotropically. Carbon atoms of the macrocation were refined anisotropically. Two out of the twelve molybdenum atoms of the POM, which existed on a rotational axis with the silicon atom, were refined anisotropically. Other molybdenum atoms were disordered and refined isotropically. Bridging oxygen atoms (Mo–O–Mo) of the POM were refined isotropically, while other oxygen atoms were refined anisotropically. Hydrogen atoms were not included in the calculation. Crystal data for **I-as**: monoclinic $P2_1/c$, $a = 22.515(3)$, $b = 18.3245(19)$, $c = 26.762(3)$, $\beta = 103.8840(16)$, $V = 10719(3)$, $Z = 4$, $R1 = 0.1539$, $wR2 = 0.3631$, $\text{Goof} = 1.068$, $\text{shift/error} = 0.000$. CCDC 1436998 contains the supplementary crystallographic data for this paper. These data are provided free of charge by the Cambridge Crystallographic Data Centre. Void analyses were carried out with a structure visualization program Mercury (CCDC) with a probe radius of 1.2 \AA . The void volume of **I-as** (1.9% of the lattice volume) was estimated after adding and optimizing the positions of hydrogen atoms. The void volume of **I-red** (1467 \AA^3 , 13.7% of the lattice volume) was estimated assuming that the lattice parameters did not change upon reduction and after removing one out of the three etpy ligands situated within the macrocation.

Acknowledgements

This work was supported by JST-PRESTO and Grant-in-Aids for Scientific Research from the Ministry of Education, Culture, Science, Sports, and Technology of Japan. Prof. Motoyuki Matsuo and Dr. Katsumi Shozugawa (Univ. of Tokyo) are acknowledged for providing access to the ICP instrument. Dr. Ryo Ishikawa and Prof. Yuuichi Ikuhara and (Univ. of Tokyo) are acknowledged for preliminary measurements with electron microscopes. Prof. Hiroshi Kageyama (Kyoto Univ.) is acknowledged for the helpful comments.

Keywords: cations · cesium · ion exchange · polyoxometalates · reduction

How to cite: *Angew. Chem. Int. Ed.* **2016**, 55, 3987–3991
Angew. Chem. **2016**, 128, 4055–4059

- [1] a) H. P. Gregor, *J. Am. Chem. Soc.* **1948**, 70, 1293; b) A. Clearfield, *Chem. Rev.* **1988**, 88, 125–148; c) J. B. Rivest, P. K. Jain, *Chem. Soc. Rev.* **2013**, 42, 89–96.
- [2] S. W. Benson, J. W. King, Jr., *Science* **1965**, 150, 1710–1713.
- [3] R. M. Barrer, L. V. C. Rees, D. J. Ward, *Proc. R. Soc. London Ser. A* **1963**, 273, 180–197.
- [4] R. D. Shannon, *Acta Crystallogr. Sect. A* **1976**, 32, 751–767.
- [5] H. S. Sherry, *J. Phys. Chem.* **1966**, 70, 1158–1168.
- [6] E. R. Nightingale, Jr., *J. Phys. Chem.* **1959**, 63, 1381–1387.
- [7] W. R. Fawcett, *J. Phys. Chem. B* **1999**, 103, 11181–11185.
- [8] T. Okuhara, *Chem. Rev.* **2002**, 102, 3641–3666.
- [9] R. M. Cornell, *J. Radioanal. Nucl. Chem.* **1993**, 171, 483–500.
- [10] a) K. Itaya, T. Ataka, S. Toshima, *J. Am. Chem. Soc.* **1982**, 104, 4767–4772; b) M. Ishizaki, S. Akiba, A. Ohtani, Y. Hoshi, K. Ono, M. Matsuba, T. Togashi, K. Kananizuka, M. Sakamoto, A. Takahashi, T. Kawamoto, H. Tanaka, M. Watanabe, M. Arisaka, T. Nankawa, M. Kurihara, *Dalton Trans.* **2013**, 42, 16049–16055.
- [11] a) S. C. Tsai, S. Ouyang, C. N. Hsu, *Appl. Radiat. Isot.* **2001**, 54, 209–215; b) M. J. Manos, M. G. Kanatzidis, *J. Am. Chem. Soc.* **2009**, 131, 6599–6607; c) R. Chitrakar, Y. Makita, A. Sonoda, *Bull. Chem. Soc. Jpn.* **2013**, 86, 1419–1425; d) D. Ding, Z. Lei, Y. Yang, C. Feng, Z. Zhang, *ACS Appl. Mater. Interfaces* **2013**, 5, 10151–10158.
- [12] a) Thematic Issue on Polyoxometalates: C. L. Hill, *Chem. Rev.* **1998**, 98, 1–390; b) Thematic Issue on Polyoxometalates: L. Cronin, A. Müller, *Chem. Soc. Rev.* **2012**, 41, 7333–7334.
- [13] A. M. Khenkin, R. Neumann, *J. Am. Chem. Soc.* **2002**, 124, 4198–4199.
- [14] N. Kawasaki, H. Weng, R. Nakanishi, S. Hamanaka, R. Kitaura, H. Shinohara, T. Yokoyama, H. Yoshikawa, K. Awaga, *Angew. Chem. Int. Ed.* **2011**, 50, 3471–3474; *Angew. Chem.* **2011**, 123, 3533–3536.
- [15] R. Kawahara, S. Uchida, N. Mizuno, *Chem. Mater.* **2015**, 27, 2092–2099.
- [16] In this work, POM with a higher anion charge ($[\alpha\text{-SiMo}_{12}\text{O}_{40}]^{4-}$) was used to increase the capacity for Cs^+ uptake. When $[\text{Cr}_3\text{O}(\text{OOCH})_6(\text{mepy})_3]^+$ was used as a macrocation, an ionic crystal with one-dimensional open channels was obtained (see the Supporting Information, Figure S1 for the crystal structure and parameters). π – π interactions between the mepy ligands probably induced formation of the one-dimensional channels. On the other hand, π – π interactions were not observed in **I-as**, which is probably because of the larger steric hindrance of the ethyl group.
- [17] Ion-exchange method: **I-as** (0.17 g, 0.05 mmol) and CsCl (1.0 g, 6.0 mmol) were added to water (50 mL), and the mixture stirred at 343 K for 12 h.

- [18] A much longer period (48 h) was needed for ion-exchange of etpyH^+ with Cs^+ at room-temperature.
- [19] Structures of **I-IE** and **I-red** could not be solved by single-crystal X-ray structure analysis (see Figure 3 for the powder XRD patterns).
- [20] Two out of the three etpy ligands in the macrocation ($[\text{Cr}_3\text{O}(\text{OOCH})_6(\text{etpy})_3]^+$) experienced anion- π interactions with $\text{C}(\text{H})-\text{O}_{\text{POM}}$ distances of 3.282 or 3.114 Å. These etpy ligands were probably fixed tightly in the crystal lattice.
- [21] In the reduction-induced ion-exchange method, **I-as** (0.17 g, 0.05 mmol), ascorbic acid (0.104 g, 0.6 mmol), and CsCl (1.7 g, 10.0 mmol) were added to water (50 mL), and the solution stirred at 343 K for 12 h. pH of the mixture was about 6.
- [22] J. Crank, *The Mathematics of Diffusion*, Oxford University Press, London, **1956**, Chapter 6.
- [23] Oxidation was carried out as follows: **I-red** (0.17 g, 0.05 mmol) was added to aqueous chlorine solution (25 mL, 0.3 %), and the aqueous solution was stirred at room-temperature for 30 min. Extending the reaction time had little effect on the degree of oxidation. Absence of chlorine in **I-ox** was confirmed with ion chromatography and XPS (Supporting Information, Figure S6).
- [24] W. Feng, T. Zhang, Y. Liu, R. Lu, C. Guan, Y. Zhao, J. Yao, *Mater. Chem. Phys.* **2003**, *77*, 294–298.
- [25] T. Noguchi, C. Chikara, K. Kuroiwa, K. Kaneko, N. Kimizuka, *Chem. Commun.* **2011**, *47*, 6455–6457.
- [26] It was confirmed that the XPS spectrum of **I-as** did not contain any peaks corresponding to Mo^{V} (Supporting Information, Figure S7).
- [27] Since protons presumably participate in the reaction, the pH of the aqueous solution was adjusted to 2 (with HCl) or 9 (with NaOH ; pH was about 6 without adjustment). At pH 2, the amount of Cs^+ uptake decreased slightly ($3.5 \text{ mol}(\text{Cs}^+) \text{ mol}(\text{s})^{-1}$) while the degree of reduction remained the same, which is probably a result of the increased amount of H^+ uptake under acidic conditions. At pH 9, the compound decomposed because of the low stability of silicododecamolybdate under basic conditions.
- [28] a) T. L. Barr, *J. Vac. Sci. Technol. A* **1991**, *9*, 1793–1805; b) J. G. Choi, L. T. Thompson, *Appl. Surf. Sci.* **1996**, *93*, 143–149.
- [29] D. M. D'Alessandro, F. R. Keene, *Chem. Soc. Rev.* **2006**, *35*, 424–440.
- [30] Compound **I-IE** has a yellow hue compared to the brown hue of **I-as**. Brown and yellow colors indicate etpy species (etpyH^+ and etpy ligand) and POM, respectively. Since etpy species are partially removed by ion-exchange, **I-IE** takes on a yellow hue.
- [31] X. López, C. Nieto-Draghi, C. Bo, J. B. Avalos, J. M. Poblet, *J. Phys. Chem. A* **2005**, *109*, 1216–1222.
- [32] R. Eguchi, S. Uchida, N. Mizuno, *Angew. Chem. Int. Ed.* **2012**, *51*, 1635–1639; *Angew. Chem.* **2012**, *124*, 1667–1671.
- [33] M. K. Johnson, D. B. Powell, R. D. Cannon, *Spectrochim. Acta Part A* **1981**, *37*, 995–1006.
- [34] C. Sanchez, J. Livage, J. P. Launay, M. Fournier, Y. Jeannin, *J. Am. Chem. Soc.* **1982**, *104*, 3194–3202.
- [35] C. Rocchiccioli-Deltcheff, M. Fournier, R. Franck, *Inorg. Chem.* **1983**, *22*, 207–216.

Received: December 15, 2015

Revised: January 22, 2016

Published online: February 19, 2016